Molecular Neurobiology (2025) 62:7998–8012
https://doi.org/10.1007/s12035-025-04771-2

RESEARCH

The Abnormal ERα-miRNA Cross-Talk in AD-Affected Human Hippocampus: A Bioinformatics Perspective

Fang-Fang Liu[1] · Ke Li[2]

Received: 4 August 2024 / Accepted: 11 February 2025 / Published online: 18 February 2025

Abstract

Estrogen's impact on Alzheimer's disease (AD) is multifaceted, with its receptors potentially influencing AD pathology in both beneficial and detrimental ways. This study aims to dissect the intricate cross-talk between estrogen receptor alpha (ERα) and microRNAs (miRNAs) in AD-affected human hippocampus. Through a comprehensive literature review in the PubMed database, coupled with a GeneCards database search, we obtained AD-related key miRNAs and genes in the hippocampus. Using bioinformatics tools, we predicted target genes and miRNAs of ERα, and the targets of the identified miRNAs. The integration of these elements resulted in the construction of an ERα-related FFL network, which includes 13 miRNAs and 56 core genes. Gene ontology (GO) and pathway enrichment analyses were conducted, revealing significant enrichment in biological processes such as neuron death and response to metal ions, and cellular components like membrane microdomains. Notably, the AKT-associated signaling pathway was prominently highlighted, with key genes including GSK3A, CDKN1A, AKT2, and MDM2, and key miRNAs including miR-485 and let-7f, suggesting a potential role of ERα in modulating this pathway in AD. The findings of this study provide a novel perspective on the regulatory network of ERα in the hippocampal region of AD and may pave the way for future research into the therapeutic potential of targeting the ERα pathway in neurodegenerative diseases.

Keywords Alzheimer's disease · Hippocampus · Estrogen · ERα · Feed-forward loops

Introduction

Alzheimer's disease (AD) is a progressive neurodegenerative disease commonly observed in the elderly population [1]. AD not only imposes significant psychological and economic burdens on patients and their families but also sees a rising societal impact and medical demand as the global population ages. It is estimated that approximately 50 million individuals worldwide are currently affected by AD or related dementias, with this number projected to increase by about 70% by the middle of this century [2].

Epidemiological studies reveal a distinct sex difference in the incidence of AD, with a higher prevalence in women compared to men [3]. This difference is associated with various factors, including the role of estrogen [4]. The estrogen receptors, ERα and ERβ, are the two primary receptors for estrogen, mediating its downstream signal transduction. Estrogen can influence the pathological processes related to AD through ERα and ERβ. Our previous studies showed that ERα and ERβ inversely regulate the levels of miR-218, leading to different alterations in the expression of its target gene, PTPα, thereby exerting distinct regulatory effects on tau pathology [5].

ERα and ERβ are transcription factors and have direct regulatory effects on a multitude of downstream genes [6]. These genes may include protein-coding genes and non-coding RNA (ncRNA) genes. It is possible that ERα and ERβ are involved in the pathological processes of AD by regulating multiple microRNAs (miRNAs). The interconnected

✉ Ke Li
likelff1@hust.edu.cn

Fang-Fang Liu
906463752@qq.com

[1] Department of Pathology, The Central Hospital of Wuhan, Tongji Medical College, Huazhong University of Science and Technology, No. 26 Shengli Street, Hankou District, Wuhan 430014, People's Republic of China

[2] Department of Blood Transfusion, Tongji Hospital, Tongji Medical College, Huazhong University of Science and Technology, No. 1095 Jiefang Avenue, Hankou District, Wuhan 430030, Hubei, People's Republic of China

feed-forward loops (FFLs) network, composed of transcription factors, miRNAs, and downstream target genes, is a common regulatory pattern in mammals [7]. The construction and analysis of FFLs serve as a valuable method for studying numerous biological regulatory processes and have been widely applied in various biological processes and diseases [8, 9].

To date, the whole FFL network of estrogen receptors has not been systematically studied or reported. The hippocampus is a significant target of estrogen action and is severely affected during the process of AD pathology. This study aims to focus on ERα, to screen and identify its target genes (including miRNAs and protein-coding genes), and to construct as well as analyze the FFL network with abnormal fluctuations centered around ERα in the hippocampus of AD patients. The findings will contribute to elucidating the complex estrogen regulatory mechanisms, identifying new markers or targets for the diagnosis and treatment of AD, and providing useful information for further experimental exploration.

Methods

Literature Search and Filter Criteria

The complete workflow employed in this study is depicted in Fig. 1. We conducted a systematic literature search for research on miRNA expression in Alzheimer's disease (AD) using the PubMed database (www.ncbi.nlm.nih.gov/pubmed/). The search terms utilized were "(microRNA OR miRNA OR miR OR micro-RNA) AND hippocamp* AND Alzheimer* AND (human OR patient*)." Original studies on the expression of miRNAs in human brain samples affected by AD were included in our study. Only articles published in peer-reviewed journals were considered for inclusion (last PubMed search date: October 1, 2023), while conference abstracts and preprint manuscripts were excluded. Additionally, miRNA studies on monogenic or familial AD were also excluded.

Identification of Key Genes Associated with AD

The GeneCards database [10] (https://www.genecards.org/) was utilized to identify key genes in the hippocampal region associated with Alzheimer's disease (AD) by searching with the keywords "alzheimer" and "hippocampus." The specific search terms used were "[all] (alzheimer) AND [all] (hippocampus)" and "[all] (alzheimer) AND [all] (hippocampal)." The search results were sorted based on relevance scores, with genes having scores greater than 10 considered key genes.

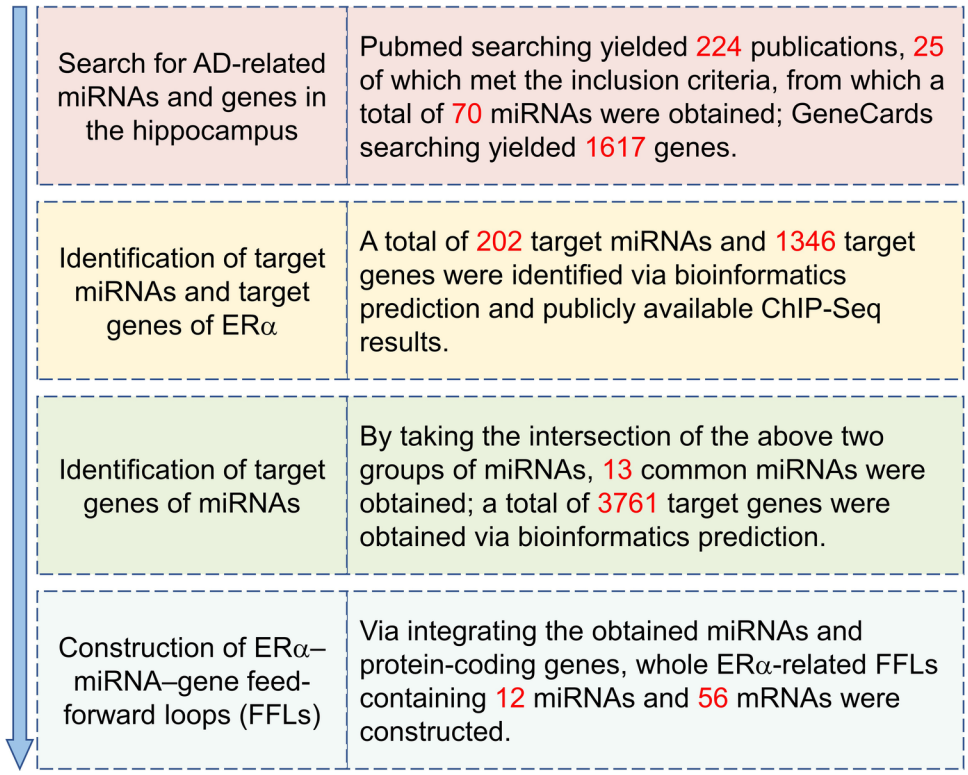

Fig. 1 Schematic workflow of this study

Identification of ERα Target Genes

In the present study, "Target genes" refer only to protein-coding genes; As for target ncRNA like miRNAs, we termed it as "target miRNAs." Four databases, Jaspar [11] (https://jaspar.elixir.no/), hTFtarget [12] (https://guolab.wchscu.cn/hTFtarget#!/), ENCODE [13] (https://maayanlab.cloud/Harmonizome/dataset/ENCODE+Transcription+Factor+Targets), and TRRUST [14] (https://www.grnpedia.org/trrust/), were used to identify target genes of ERα. Genes predicted in at least two of the four databases were considered eligible target genes.

Identification of ERα Target miRNAs

The Identification of target miRNAs is relatively more challenging compared to target genes, primarily due to the uncertain regulatory location of ERα on miRNAs. Some miRNAs are located within coding regions, while others are in non-coding regions. It is difficult to determine whether ERα regulation occurs upstream of the genomic location where the miRNA is situated or upstream of the gene that encodes it. Therefore, this study adopted a more stringent screening approach: three databases were used to identify potential downstream target miRNAs of ERα, namely TransmiR v2.0 [15] (https://www.cuilab.cn/transmir), mirTrans [16] (http://123.207.219.84/mirtrans/), and hTFtarget [12] (https://guolab.wchscu.cn/hTFtarget#!/). Only those miRNAs predicted in all three databases were considered meeting the criteria for target miRNAs.

Identification of Target Genes of miRNAs

A total of seven tools or databases, RNA22 [17] (https://cm.jefferson.edu/rna22/), DIANA-microT 2023 [18] (www.microrna.gr/microt_webserver/), miRanda [19] (http://www.microrna.org), TargetScanHuman (version: 8.0) [20] (https://www.targetscan.org/vert_80/), miRmap [21] (http://mirmap.ezlab.org), PITA [22] (http://genie.weizmann.ac.il/pubs/mir07), and PicTar [23] (https://pictar.mdc-berlin.de/), were used to predict target genes of miRNAs. Genes successfully predicted by at least three of these tools were considered fulfilling the criteria for target genes.

Protein–Protein Interaction (PPI) Network Enrichment Analysis

Genes were uploaded to the STRING database [24] (Version: 12; https://string-db.org/) to predict the interactions among proteins encoded by these genes. The PPI network was subsequently built and visualized by Cytoscape (version: 3.8.2) [25]. The Molecular Complex Detection (MCODE) algorithm in the MCODE app of Cytoscape was used to identify densely connected network nodes. The identified highly interconnected regions were termed as the core cluster. Node Score Cutoff (NSC) and *k*-core were the most influential parameters for cluster size in the MCODE algorithm. NSC controls the minimum score required for a node to be included in a cluster. Smaller NSC values allow for larger clusters, while higher values create smaller clusters. For example, an NSC of 0.5 means that new members' node scores must be no more than 50% less than that of the seed node. In the present study, we set the NSC to 0.2 to ensure that only nodes with strong connectivity within the network are included in the core cluster. The *k*-core ensures that each node within a cluster is connected to at least k other nodes within the same cluster. The *k*-core parameter filters out clusters that do not contain a maximally inter-connected sub-cluster of at least k degrees. For instance, a *k*-core value of 2 means that each node in the cluster must be connected to at least two other nodes. In this study, we set the *k*-core to 2 to ensure that the identified clusters are robust and highly interconnected.

Gene Ontology (GO) Analysis and Pathway Enrichment Analysis

GO analysis and Kyoto Encyclopedia of Genes and Genomes (KEGG) pathway enrichment analysis were conducted using R package "clusterProfiler" (Version: 4.2.2) [26–28]. Reactome pathway enrichment analysis was performed using R package "ReactomePA" (Version: 1.42.0) [29] or "WebGestaltR" (0.4.6) [30]. The false discovery rate (FDR) < 0.05 was set as the cut-off criterion. For GO analysis, R package "rrvgo" (Version: 1.14.2) [31] was used to reduce and summarize identified GO terms to their parent GO terms by identifying redundance based on semantic similarity.

Results

Retrieving Differentially Expressed miRNAs in the Hippocampus of AD Patients

The workflow and entire procedures of this study were delineated in Fig. 1, beginning with the identification of differentially expressed miRNAs within the hippocampus in AD. The systematic literature search was conducted in the PubMed database using specific search terms, yielding a total of 224 publications, of which 25 original research articles that included human brain data from AD patients were classified as eligible for inclusion. From these 25 original studies, we extracted a total of 81 differentially expressed miRNAs (DEmiRNAs) (Table 1). Among these 81 miRNAs, 49 were upregulated and 43 were downregulated in AD-affected human hippocampus.

Table 1 Metadata of deregulated miRNA in AD hippocampus extracted from previous studies (current until Oct 1, 2023)

PMID	Year	Corresponding author	Diagnosis	Sample (origin country)	Sample size	Tissue	miRNA	miRBASE ID	Changes in AD
24,014,289	2013	Bart De Strooper	AD	UK	AD, $n=41$; Ctrl, $n=23$	Hippocampus	hsa-let-7f-5p	MIMAT0000067	up
24,014,289	2013	Bart De Strooper	AD	UK	AD, $n=41$; Ctrl, $n=23$	Hippocampus	hsa-let-7i-5p	MIMAT0000415	up
23,962,497	2014	Marcel M Verbeek	AD; Braak III/IV	Netherlands	AD, $n=10$; Ctrl, $n=11$	Hippocampus	hsa-miR-107	MIMAT0000104	up
27,298,190	2016	Maria-Adelaide Micci	AD	USA	AD, $n=6$; Ctrl, $n=4$	Hippocampus	hsa-miR-124-3p	MIMAT0000422	up
28,965,984	2018	Ling-Qiang Zhu	AD	Canada	AD, $n=8$; Ctrl, $n=8$	Hippocampus	hsa-miR-124-3p	MIMAT0000422	up
17,314,675	2007	Walter J Lukiw	AD	USA, Canada	AD, $n=5$; Ctrl, $n=5$	Hippocampal CA1	hsa-miR-125b-5p	MIMAT0000423	up
18,525,125	2008	Cynthia A Richards	AD; Braak V/VI	Netherlands	AD, $n=10$; Ctrl, $n=7$	Hippocampus	hsa-miR-125b-5p	MIMAT0000423	up
23,462,268	2013	Walter J Lukiw	AD	USA	AD, $n=3$; Ctrl, $n=3$	hippocampus CA1	hsa-miR-125b-5p	MIMAT0000423	up
17,314,675	2007	Walter J Lukiw	AD	USA, Canada	AD, $n=5$; Ctrl, $n=5$	Hippocampal CA1	hsa-miR-128-3p	MIMAT0000424	up
23,962,497	2014	Marcel M Verbeek	AD; Braak III/IV	Netherlands	AD, $n=10$; Ctrl, $n=11$	Hippocampus	hsa-miR-128-3p	MIMAT0000424	up
27,298,190	2016	Maria-Adelaide Micci	AD	USA	AD, $n=6$; Ctrl, $n=4$	Hippocampus	hsa-miR-132-3p	MIMAT0000426	up
27,298,190	2016	Maria-Adelaide Micci	AD	USA	AD, $n=6$; Ctrl, $n=4$	Hippocampus	hsa-miR-137	MIMAT0000429	up
29,253,717	2017	Lynn M Bekris	AD	USA	AD, $n=21$; Ctrl, $n=22$	hippocampus	hsa-miR-140-5p	MIMAT0000431	up
24,014,289	2013	Bart De Strooper	AD	UK	AD, $n=41$; Ctrl, $n=23$	Hippocampus	hsa-miR-142-3p	MIMAT0000434	up
30,314,521	2018	Bart De Strooper	AD	UK	AD, $n=28$; Ctrl, $n=20$	Hippocampus	hsa-miR-142-5p	MIMAT0000433	up
28,871,468	2017	Isidro Ferrer	AD; Braak III-IV	Spain	AD, $n=25$; Ctrl, $n=19$	hippocampus CA1	hsa-miR-143-3p	MIMAT0000435	up
18,525,125	2008	Cynthia A Richards	AD; Braak V/VI	Netherlands	AD, $n=10$; Ctrl, $n=7$	Hippocampus	hsa-miR-145-5p	MIMAT0000437	up
18,801,740	2008	Jian Guo Cui	AD	USA, Canada	AD, $n=23$; Ctrl, $n=23$	Hippocampus	hsa-miR-146a-5p	MIMAT0000449	up
20,937,840	2010	Walter J Lukiw	AD	USA	AD, $n=16$; Ctrl, $n=16$	Hippocampus	hsa-miR-146a-5p	MIMAT0000449	up
23,462,268	2013	Walter J Lukiw	AD	USA	AD, $n=3$; Ctrl, $n=3$	hippocampus CA1	hsa-miR-146a-5p	MIMAT0000449	up
23,962,497	2014	Marcel M Verbeek	AD; Braak III/IV	Netherlands	AD, $n=10$; Ctrl, $n=11$	Hippocampus	hsa-miR-146a-5p	MIMAT0000449	up
27,929,395	2016	Walter J Lukiw	AD	USA	AD, $n=12$; Ctrl, $n=6$	hippocampus CA1	hsa-miR-146a-5p	MIMAT0000449	up
30,314,521	2018	Bart De Strooper	AD	UK	AD, $n=28$; Ctrl, $n=20$	Hippocampus	hsa-miR-146a-5p	MIMAT0000449	up
24,014,289	2013	Bart De Strooper	AD	UK	AD, $n=41$; Ctrl, $n=23$	Hippocampus	hsa-miR-150-5p	MIMAT0000451	up
23,462,268	2013	Walter J Lukiw	AD	USA	AD, $n=3$; Ctrl, $n=3$	hippocampus CA1	hsa-miR-155-5p	MIMAT0000646	up
30,314,521	2018	Bart De Strooper	AD	UK	AD, $n=28$; Ctrl, $n=20$	Hippocampus	hsa-miR-155-5p	MIMAT0000646	up
23,962,497	2014	Marcel M Verbeek	AD; Braak III/IV	Netherlands	AD, $n=10$; Ctrl, $n=11$	Hippocampus	hsa-miR-16-5p	MIMAT0000069	up

Table 1 (continued)

PMID	Year	Corresponding author	Diagnosis	Sample (origin country)	Sample size	Tissue	miRNA	miRBASE ID	Changes in AD
29,253,717	2017	Lynn M Bekris	AD	USA	AD, $n=21$; Ctrl, $n=22$	hippocampus	hsa-miR-182-5p	MIMAT0000259	up
23,462,268	2013	Walter J Lukiw	AD	USA	AD, $n=3$; Ctrl, $n=3$	hippocampus CA1	hsa-miR-183-5p	MIMAT0000261	up
29,253,717	2017	Lynn M Bekris	AD	USA	AD, $n=21$; Ctrl, $n=22$	hippocampus	hsa-miR-194-5p	MIMAT0000460	up
24,014,289	2013	Bart De Strooper	AD	UK	AD, $n=41$; Ctrl, $n=23$	Hippocampus	hsa-miR-195-5p	MIMAT0000461	up
24,014,289	2013	Bart De Strooper	AD	UK	AD, $n=41$; Ctrl, $n=23$	Hippocampus	hsa-miR-199a-3p	MIMAT0000232	up
24,014,289	2013	Bart De Strooper	AD	UK	AD, $n=41$; Ctrl, $n=23$	Hippocampus	hsa-miR-199a-3p	MIMAT0000232	up
24,014,289	2013	Bart De Strooper	AD	UK	AD, $n=41$; Ctrl, $n=23$	Hippocampus	hsa-miR-200a-3p	MIMAT0000682	up
18,525,125	2008	Cynthia A Richards	AD; Braak V/VI	Netherlands	AD, $n=10$; Ctrl, $n=7$	Hippocampus	hsa-miR-214-3p	MIMAT0000271	up
24,014,289	2013	Bart De Strooper	AD	UK	AD, $n=41$; Ctrl, $n=23$	Hippocampus	hsa-miR-223-3p	MIMAT0000280	up
24,014,289	2013	Bart De Strooper	AD	UK	AD, $n=41$; Ctrl, $n=23$	Hippocampus	hsa-miR-23a-3p	MIMAT0000078	up
27,298,190	2016	Maria-Adelaide Micci	AD	USA	AD, $n=6$; Ctrl, $n=4$	Hippocampus	hsa-miR-25-3p	MIMAT0000081	up
24,014,289	2013	Bart De Strooper	AD	UK	AD, $n=41$; Ctrl, $n=23$	Hippocampus	hsa-miR-27a-3p	MIMAT0000084	up
18,525,125	2008	Cynthia A Richards	AD; Braak V/VI	Netherlands	AD, $n=10$; Ctrl, $n=7$	Hippocampus	hsa-miR-27b-3p	MIMAT0000419	up
18,525,125	2008	Cynthia A Richards	AD; Braak V/VI	Netherlands	AD, $n=10$; Ctrl, $n=7$	Hippocampus	hsa-miR-296-5p	MIMAT0000690	up
27,298,190	2016	Maria-Adelaide Micci	AD	USA	AD, $n=6$; Ctrl, $n=4$	Hippocampus	hsa-miR-29a-3p	MIMAT0000086	up
30,522,932	2019	Chu Chen	AD	USA	AD, $n=15$; Ctrl, $n=14$	Hippocampus	hsa-miR-30b-5p	MIMAT0000420	up
31,134,481	2021	Peigang Cao	AD	China	AD, $n=8$; Ctrl, $n=5$	Hippocampus	hsa-miR-342-3p	MIMAT0000753	up
18,525,125	2008	Cynthia A Richards	AD; Braak V/VI	Netherlands	AD, $n=10$; Ctrl, $n=7$	Hippocampus	hsa-miR-346	MIMAT0000773	up
22,160,687	2011	Gerry Melino	AD; Braak V/VI	UK	AD, $n=29$; Ctrl, $n=20$	Hippocampus	hsa-miR-34a-5p	MIMAT0000255	up
23,462,268	2013	Walter J Lukiw	AD	USA	AD, $n=3$; Ctrl, $n=3$	hippocampus CA1	hsa-miR-34a-5p	MIMAT0000255	up
23,962,497	2014	Marcel M Verbeek	AD; Braak III/IV	Netherlands	AD, $n=10$; Ctrl, $n=11$	Hippocampus	hsa-miR-34a-5p	MIMAT0000255	up
23,962,497	2014	Marcel M Verbeek	AD; Braak VI	Netherlands	AD, $n=10$; Ctrl, $n=11$	Hippocampus	hsa-miR-34a-5p	MIMAT0000255	up
23,962,497	2014	Marcel M Verbeek	AD; Braak III/IV	Netherlands	AD, $n=10$; Ctrl, $n=11$	Hippocampus	hsa-miR-34c-5p	MIMAT0000686	up
24,014,289	2013	Bart De Strooper	AD	UK	AD, $n=41$; Ctrl, $n=23$	Hippocampus	hsa-miR-362-3p	MIMAT0004683	up
24,014,289	2013	Bart De Strooper	AD	UK	AD, $n=41$; Ctrl, $n=23$	Hippocampus	hsa-miR-363-3p	MIMAT0000707	up
18,525,125	2008	Cynthia A Richards	AD; Braak V/VI	Netherlands	AD, $n=10$; Ctrl, $n=7$	Hippocampus	hsa-miR-422a	MIMAT0001339	up
18,525,125	2008	Cynthia A Richards	AD; Braak V/VI	Netherlands	AD, $n=10$; Ctrl, $n=7$	Hippocampus	hsa-miR-423-3p	MIMAT0001340	up

Table 1 (continued)

PMID	Year	Corresponding author	Diagnosis	Sample (origin country)	Sample size	Tissue	miRNA	miRBASE ID	Changes in AD
18,525,125	2008	Cynthia A Richards	AD; Braak V/VI	Netherlands	AD, $n=10$; Ctrl, $n=7$	Hippocampus	hsa-miR-451a	MIMAT0001631	up
24,014,289	2013	Bart De Strooper	AD	UK	AD, $n=41$; Ctrl, $n=23$	Hippocampus	hsa-miR-455-5p	MIMAT0003150	up
30,314,521	2018	Bart De Strooper	AD	UK	AD, $n=28$; Ctrl, $n=20$	Hippocampus	hsa-miR-455-5p	MIMAT0003150	up
18,525,125	2008	Cynthia A Richards	AD; Braak V/VI	Netherlands	AD, $n=10$; Ctrl, $n=7$	Hippocampus	hsa-miR-501-5p	MIMAT0002872	up
18,525,125	2008	Cynthia A Richards	AD; Braak V/VI	Netherlands	AD, $n=10$; Ctrl, $n=7$	Hippocampus	hsa-miR-505-3p	MIMAT0002876	up
18,525,125	2008	Cynthia A Richards	AD; Braak V/VI	Netherlands	AD, $n=10$; Ctrl, $n=7$	Hippocampus	hsa-miR-514a-3p	MIMAT0002883	up
26,856,603	2016	Yun Wang	AD	China	AD, $n=7$; Ctrl, $n=7$	Hippocampus	hsa-miR-603	MIMAT0003271	up
18,525,125	2008	Cynthia A Richards	AD; Braak V/VI	Netherlands	AD, $n=10$; Ctrl, $n=7$	Hippocampus	hsa-miR-92a-3p	MIMAT0000092	up
24,014,289	2013	Bart De Strooper	AD	UK	AD, $n=41$; Ctrl, $n=23$	Hippocampus	hsa-miR-92b-3p	MIMAT0003218	up
17,314,675	2007	Walter J Lukiw	AD	USA, Canada	AD, $n=5$; Ctrl, $n=5$	Hippocampal CA1	hsa-miR-9-5p	MIMAT0000441	up
27,298,190	2016	Maria-Adelaide Micci	AD	USA	AD, $n=6$; Ctrl, $n=4$	Hippocampus	hsa-miR-9-5p	MIMAT0000441	up
18,525,125	2008	Cynthia A Richards	AD; Braak V/VI	Netherlands	AD, $n=10$; Ctrl, $n=7$	Hippocampus	hsa-miR-103a-3p	MIMAT0000101	down
23,962,497	2014	Marcel M Verbeek	AD; Braak VI	Netherlands	AD, $n=10$; Ctrl, $n=11$	Hippocampus	hsa-miR-107	MIMAT0000104	down
17,314,675	2007	Walter J Lukiw	AD	USA, Canada	AD, $n=5$; Ctrl, $n=5$	Hippocampal CA1	hsa-miR-124-3p	MIMAT0000422	down
24,014,289	2013	Bart De Strooper	AD	UK	AD, $n=41$; Ctrl, $n=23$	Hippocampus	hsa-miR-124-3p	MIMAT0000422	down
28,871,468	2017	Isidro Ferrer	AD; Braak III-IV	Spain	AD, $n=25$; Ctrl, $n=19$	hippocampus CA1	hsa-miR-124-3p	MIMAT0000422	down
29,253,717	2017	Lynn M Bekris	AD	USA	AD, $n=21$; Ctrl, $n=22$	hippocampus	hsa-miR-126-3p	MIMAT0000445	down
24,014,289	2013	Bart De Strooper	AD	UK	AD, $n=41$; Ctrl, $n=23$	Hippocampus	hsa-miR-127-3p	MIMAT0000446	down
23,962,497	2014	Marcel M Verbeek	AD; Braak VI	Netherlands	AD, $n=10$; Ctrl, $n=11$	Hippocampus	hsa-miR-128-3p	MIMAT0000424	down
24,014,289	2013	Bart De Strooper	AD	UK	AD, $n=41$; Ctrl, $n=23$	Hippocampus	hsa-miR-128-3p	MIMAT0000424	down
24,014,289	2013	Bart De Strooper	AD	UK	AD, $n=41$; Ctrl, $n=23$	Hippocampus	hsa-miR-129–2-3p	MIMAT0004605	down
24,014,289	2013	Bart De Strooper	AD	UK	AD, $n=41$; Ctrl, $n=23$	Hippocampus	hsa-miR-129-5p	MIMAT0000242	down
18,525,125	2008	Cynthia A Richards	AD; Braak V/VI	Netherlands	AD, $n=10$; Ctrl, $n=7$	Hippocampus	hsa-miR-132-3p	MIMAT0000426	down
24,014,289	2013	Bart De Strooper	AD	UK	AD, $n=41$; Ctrl, $n=23$	Hippocampus	hsa-miR-132-3p	MIMAT0000426	down
26,362,250	2015	Sébastien S Hébert	AD	Canada	AD, $n=10$; Ctrl, $n=13$	Hippocampus	hsa-miR-132-3p	MIMAT0000426	down
28,871,468	2017	Isidro Ferrer	AD; Braak III-IV	Spain	AD, $n=25$; Ctrl, $n=19$	hippocampus CA1	hsa-miR-132-3p	MIMAT0000426	down
29,855,513	2018	D Gurwitz	AD	UK	AD, $n=14$; Ctrl, $n=20$	hippocampus	hsa-miR-132-3p	MIMAT0000426	down

Table 1 (continued)

PMID	Year	Corresponding author	Diagnosis	Sample (origin country)	Sample size	Tissue	miRNA	miRBASE ID	Changes in AD
34,033,742	2021	Evgenia Salta	AD	Belgium, Sweden	AD, $n=10$; Ctrl, $n=10$	Hippocampus	hsa-miR-132-3p	MIMAT0000426	down
29,523,845	2018	Anna Maria D'Erchia	AD; Braak V-VI	USA, UK	AD, $n=6$; Ctrl, $n=6$	hippocampus	hsa-miR-132-5p	MIMAT0004594	down
24,014,289	2013	Bart De Strooper	AD	UK	AD, $n=41$; Ctrl, $n=23$	Hippocampus	hsa-miR-136-5p	MIMAT0000448	down
24,014,289	2013	Bart De Strooper	AD	UK	AD, $n=41$; Ctrl, $n=23$	Hippocampus	hsa-miR-138-5p	MIMAT0000430	down
35,887,339	2022	Tae Ho Lee	AD	China	AD, $n=6$; Ctrl, $n=5$	Hippocampus	hsa-miR-143-3p	MIMAT0000435	down
23,962,497	2014	Marcel M Verbeek	AD; Braak VI	Netherlands	AD, $n=10$; Ctrl, $n=11$	Hippocampus	hsa-miR-146a-5p	MIMAT0000449	down
18,525,125	2008	Cynthia A Richards	AD; Braak V/VI	Netherlands	AD, $n=10$; Ctrl, $n=7$	Hippocampus	hsa-miR-146b-5p	MIMAT0002809	down
23,962,497	2014	Marcel M Verbeek	AD; Braak VI	Netherlands	AD, $n=10$; Ctrl, $n=11$	Hippocampus	hsa-miR-16-5p	MIMAT0000069	down
29,523,845	2018	Anna Maria D'Erchia	AD; Braak V-VI	USA, UK	AD, $n=6$; Ctrl, $n=6$	hippocampus	hsa-miR-184	MIMAT0000454	down
18,525,125	2008	Cynthia A Richards	AD; Braak V/VI	Netherlands	AD, $n=10$; Ctrl, $n=7$	Hippocampus	hsa-miR-210-3p	MIMAT0000267	down
29,855,513	2018	D Gurwitz	AD	UK	AD, $n=14$; Ctrl, $n=20$	hippocampus	hsa-miR-212	MIMAT0000269	down
18,525,125	2008	Cynthia A Richards	AD; Braak V/VI	Netherlands	AD, $n=10$; Ctrl, $n=7$	Hippocampus	hsa-miR-212-3p	MIMAT0000269	down
23,408,966	2013	Yan Zhang	AD	USA	AD, $n=8$; Ctrl, $n=8$	Hippocampus	hsa-miR-214-3p	MIMAT0000271	down
24,014,289	2013	Bart De Strooper	AD	UK	AD, $n=41$; Ctrl, $n=23$	Hippocampus	hsa-miR-219a-2-3p	MIMAT0004675	down
18,525,125	2008	Cynthia A Richards	AD; Braak V/VI	Netherlands	AD, $n=10$; Ctrl, $n=7$	Hippocampus	hsa-miR-219a-5p	MIMAT0000276	down
28,871,468	2017	Isidro Ferrer	AD; Braak III-IV	Spain	AD, $n=25$; Ctrl, $n=19$	hippocampus CA1	hsa-miR-27a-3p	MIMAT0000084	down
24,014,289	2013	Bart De Strooper	AD	UK	AD, $n=41$; Ctrl, $n=23$	Hippocampus	hsa-miR-329-3p	MIMAT0001629	down
30,576,233	2019	Guo-Ping Peng	AD	USA	AD, $n=12$; Ctrl, $n=11$	Hippocampus	hsa-miR-338-5p	MIMAT0004701	down
29,523,845	2018	Anna Maria D'Erchia	AD; Braak V-VI	USA, UK	AD, $n=6$; Ctrl, $n=6$	hippocampus	hsa-miR-34c-3p	MIMAT0004677	down
23,962,497	2014	Marcel M Verbeek	AD; Braak VI	Netherlands	AD, $n=10$; Ctrl, $n=11$	Hippocampus	hsa-miR-34c-5p	MIMAT0000686	down
24,014,289	2013	Bart De Strooper	AD	UK	AD, $n=41$; Ctrl, $n=23$	Hippocampus	hsa-miR-370-3p	MIMAT0000722	down
29,523,845	2018	Anna Maria D'Erchia	AD; Braak V-VI	USA, UK	AD, $n=6$; Ctrl, $n=6$	hippocampus	hsa-miR-375-3p	MIMAT0000728	down
18,525,125	2008	Cynthia A Richards	AD; Braak V/VI	Netherlands	AD, $n=10$; Ctrl, $n=7$	Hippocampus	hsa-miR-382-5p	MIMAT0000737	down
24,014,289	2013	Bart De Strooper	AD	UK	AD, $n=41$; Ctrl, $n=23$	Hippocampus	hsa-miR-409-5p	MIMAT0001638	down
24,014,289	2013	Bart De Strooper	AD	UK	AD, $n=41$; Ctrl, $n=23$	Hippocampus	hsa-miR-410-3p	MIMAT0002171	down
18,525,125	2008	Cynthia A Richards	AD; Braak V/VI	Netherlands	AD, $n=10$; Ctrl, $n=7$	Hippocampus	hsa-miR-425-5p	MIMAT0003393	down
24,014,289	2013	Bart De Strooper	AD	UK	AD, $n=41$; Ctrl, $n=23$	Hippocampus	hsa-miR-425-5p	MIMAT0003393	down

Table 1 (continued)

PMID	Year	Corresponding author	Diagnosis	Sample (origin country)	Sample size	Tissue	miRNA	miRBASE ID	Changes in AD
24,014,289	2013	Bart De Strooper	AD	UK	AD, $n=41$; Ctrl, $n=23$	Hippocampus	hsa-miR-433-3p	MIMAT0001627	down
20,507,594	2010	Claes Wahlestedt	AD	USA	AD, $n=35$; Ctrl, $n=35$	Hippocampus	hsa-miR-485-5p	MIMAT0002175	down
24,014,289	2013	Bart De Strooper	AD	UK	AD, $n=41$; Ctrl, $n=23$	Hippocampus	hsa-miR-487a-3p	MIMAT0002178	down
24,014,289	2013	Bart De Strooper	AD	UK	AD, $n=41$; Ctrl, $n=23$	Hippocampus	hsa-miR-487b-3p	MIMAT0003180	down
24,014,289	2013	Bart De Strooper	AD	UK	AD, $n=41$; Ctrl, $n=23$	Hippocampus	hsa-miR-495-3p	MIMAT0002817	down
24,014,289	2013	Bart De Strooper	AD	UK	AD, $n=41$; Ctrl, $n=23$	Hippocampus	hsa-miR-543	MIMAT0004954	down
24,014,289	2013	Bart De Strooper	AD	UK	AD, $n=41$; Ctrl, $n=23$	Hippocampus	hsa-miR-769-5p	MIMAT0003886	down
23,962,497	2014	Marcel M Verbeek	AD; Braak III/IV	Netherlands	AD, $n=10$; Ctrl, $n=11$	Hippocampus	hsa-miR-9-3p	MIMAT0000442	down
23,962,497	2014	Marcel M Verbeek	AD; Braak VI	Netherlands	AD, $n=10$; Ctrl, $n=11$	Hippocampus	hsa-miR-9-3p	MIMAT0000442	down
18,525,125	2008	Cynthia A Richards	AD; Braak V/VI	Netherlands	AD, $n=10$; Ctrl, $n=7$	Hippocampus	hsa-miR-9-5p	MIMAT0000441	down

However, discordant expression patterns were observed for 11 miRNAs, which showed inconsistent results across different studies—upregulated in one and downregulated in another. This discrepancy does not necessarily indicate flawed research findings but may be associated with differences in the specific hippocampal subregions examined in the original studies or differences in the Braak stage of the AD patients. To maintain consistency, and in the absence of relevant details, these 11 miRNAs were still excluded from subsequent calculations in this study despite the strong likelihood that they too were DEmiRNAs and play significant roles in AD. The excluded miRNAs were as follows: hsa-miR-107, hsa-miR-124-3p, hsa-miR-128-3p, hsa-miR-132-3p, hsa-miR-143-3p, hsa-miR-146a-5p, hsa-miR-16-5p, hsa-miR-214-3p, hsa-miR-27a-3p, hsa-miR-34c-5p, and hsa-miR-9-5p. Finally, 38 upregulated and 32 downregulated miRNAs were obtained.

Prediction of ERα Target miRNAs

In this study, we employed a trio of databases—TransmiR, mirTrans, and hTFtarget—to collaboratively predict the downstream miRNAs of ERα. From these databases, we obtained 411 miRNAs (Supplementary Table 1), 1020 miRNAs (Supplementary Table 2), and 1882 miRNAs (Supplementary Table 3), respectively. After converting the miRNA gene symbols from these results to their official names in the miRBase database, we intersected them with the 70 miRNAs obtained above and obtained 13 common miRNAs, with 5 being upregulated and 8 being downregulated in AD (Fig. 2A and Table 2).

Prediction of Target Genes for the 13 Common miRNAs

To enhance the accuracy of results, we employed a total of seven bioinformatic tools or databases to identify the downstream targets for the 13 common miRNAs: microT, miRanda, TargetScan, PITA, RNA22, miRmap, and PicTar. We set a relatively stringent criterion for target gene selection, requiring that a gene be successfully predicted in at least three of the seven databases to be considered a valid target. Finally, 3761 genes were acquired (Fig. 2B and Supplementary Table 4). Subsequent analysis of the prediction results revealed that among these 13 miRNAs, the top five in terms of the number of downstream targets are as follows: hsa-miR-410-3p (1133 target genes), hsa-let-7f-5p (781 target genes), hsa-miR-25-3p (715 target genes), hsa-miR-485-5p (618 target genes), and hsa-miR-194-5p (555 target genes).

Prediction of ERα Target Genes

The prediction of target genes (protein-coding genes) downstream of transcription factors is considerably more advanced and accurate compared to the prediction of target miRNAs. We utilized four databases to predict the downstream target genes of ERα. These databases include Jaspar,

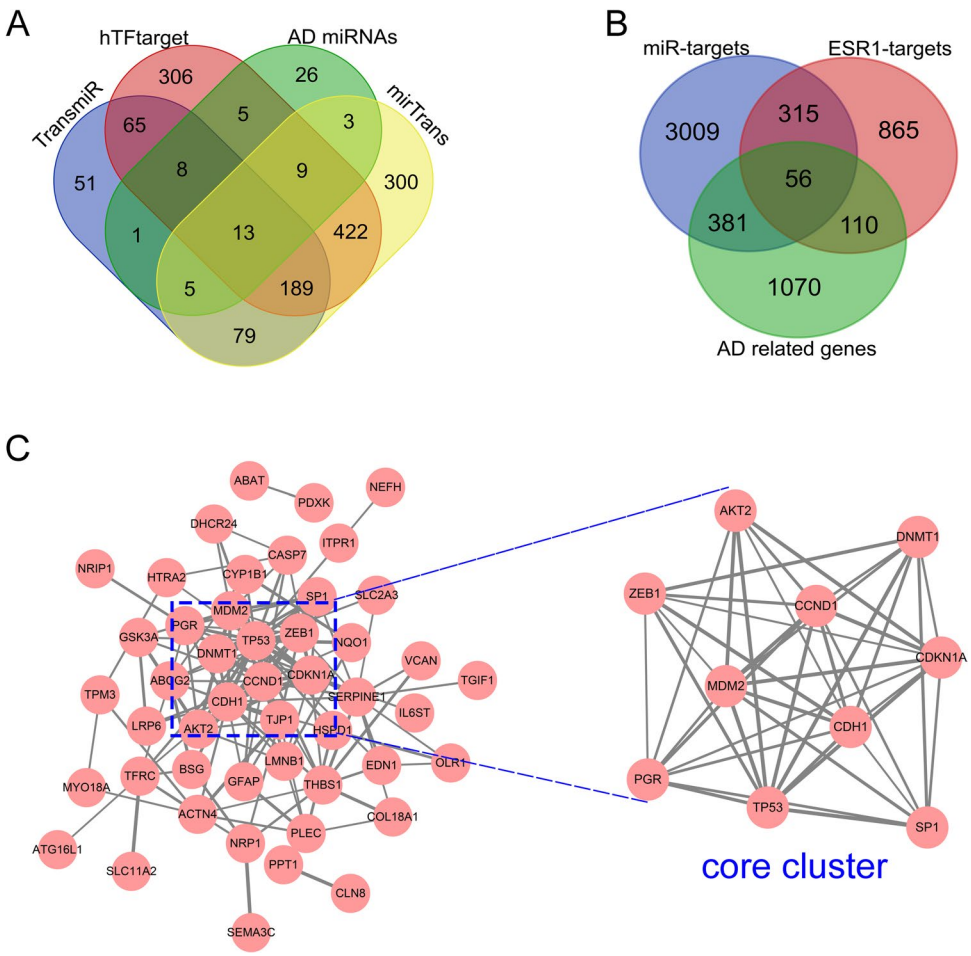

Fig. 2 Identification of common miRNAs and genes in AD-affected hippocampus. **A** Venn diagram showing the intersection of miRNAs obtained from AD-related studies with those predicted as targets of ERα from the databases TransmiR, mirTrans, and hTFtarget. **B** Venn diagram of the identified target genes for the 13 common miRNAs, ERα target genes and AD-related genes. **C** PPI network analysis revealing a core cluster of 10 genes with robust interactions

hTFtarget, ENCODE, and TRRUST. Only genes that were successfully predicted in at least two of these databases were considered targets of ERα. This approach resulted in a final set of 1346 genes (Fig. 2B and Supplementary Table 5).

Retrieval and Selection of Genes Highly Associated with AD in the Hippocampus

Initially, we attempted to identify differentially expressed genes (DEGs) in the hippocampal region of AD using publicly available datasets from microarray and high throughput sequencing. However, results obtained from the analysis of these datasets exhibited considerable inconsistency, making it challenging to integrate DEGs across different datasets. Moreover, attempting to forcibly remove batch effects when combining multiple datasets from different experimental platforms, while yielding some DEGs, resulted in a dramatically reduced number of them (data not shown).

Consequently, we discarded this method of gene screening/identification and instead opted to utilize the GeneCards database for the search and selection of genes related to AD in the hippocampal region. Employing a defined search strategy and selection criteria, we identified a total of 1617 genes (Fig. 2B and Supplementary Table 6). This approach provided a more reasonable and extensive list of genes that are potentially implicated in AD pathology in the hippocampus.

Identification of Common Genes and PPI Network Analysis

By integrating the above target prediction results, we identified 56 common genes (Fig. 2B and Supplementary Table 7). These 56 genes are not only important genes related to AD pathology in the hippocampal region but are also targets of ERα and the 13 identified common miRNAs. To further understand the biological significance of the 56 core genes, we performed GO and pathway enrichment analysis (KEGG pathway and Reactome pathway). The GO analysis revealed several enriched terms. Specifically, in the BP aspect, the top three enriched GO terms were "response to metal ion," "neuron death," and "neuron apoptotic process"; In the CC aspect, the top three enriched GO terms were "membrane raft," "membrane microdomain," and "platelet alpha granule lumen"; In the MF aspect, the top three enriched GO terms were "histone deacetylase binding," "histone acetyltransferase binding," and "structural constituent of cytoskeleton"

Table 2 Thirteen predicted miRNAs regulated by ESR1 (ERα). The "Z-score" (TransmiR) is defined as the number of standard deviations above the mean raw score of the other regions within the miRNA promoter; The "Affinity score" (mirTrans) describes the binding strength of the TF to the transcription factor binding sites (TFBS)

miRNA symbol	miRBASE ID	TransmiR Z-score	mirTrans Affinity score	hTFtarget (Chip-seq) No. of TSS peaks (total/average; the peak with strongest signal; tissue)	Changes in AD
hsa-let-7f-5p	MIMAT0000067	2.18	0.73	21/1; Chr9,94,165,515,94,167,230,44.0,−108,pr,data set-4693; breast	Up
hsa-miR-194-5p	MIMAT0000460	1.9	0.999	117/2; Chr11,64,893,790,64,895,154,349.,−371,pr,data set-4001; breast	Up
hsa-miR-25-3p	MIMAT0000081	2.59	0.703	58/1; Chr7,100,100,365,100,100,889,112.,−724,pr,data set-4178; breast	Up
hsa-miR-342-3p	MIMAT0000753	2.26	0.984	135/1; Chr14,100,108,100,100,108,934,316.,−155,pr,data set-4001; breast	Up
hsa-miR-455-5p	MIMAT0003150	2.11	0.697	65/1; Chr9,114,206,966,114,207,496,62.1,−245,pr,data set-3931; breast	Up
hsa-miR-210-3p	MIMAT0000267	1.87	1	103/1; Chr11,569,241,569,958,88.0,−176,pr,dataset-1114; breast	Down
hsa-miR-382-5p	MIMAT0000737	2.09	0.751	28/2; Chr14,101,063,988,101,064,461,91.7,−100,pr,data set-4001; breast	Down
hsa-miR-409-5p	MIMAT0001638	2.09	0.751	32/1; Chr14,101,063,988,101,064,461,91.7,−130,pr,data set-4001; breast	Down
hsa-miR-410-3p	MIMAT0002171	2.09	0.751	35/1; Chr14,101,063,988,101,064,461,91.7,−190,pr,data set-4001; breast	Down
hsa-miR-425-5p	MIMAT0003393	2.77	0.994	103/2; Chr3,49,021,681,49,022,497,353.,−226,pr,data set-4001; breast	Down
hsa-miR-485-5p	MIMAT0002175	2.09	0.751	31/2; Chr14,101,053,762,101,054,048,9.50,−164,pr,data set-4681; BREAST	Down
hsa-miR-487a-3p	MIMAT0002178	2.09	0.751	29/2; Chr14,101,049,961,101,050,146,9.02,−246,pr,data set-5292; breast	Down
hsa-miR-487b-3p	MIMAT0003180	2.09	0.751	26/2; Chr14,101,039,443,101,039,714,14.9,−699,pr,data set-4693; breast	Down

(Supplementary Table 8). The KEGG pathway enrichment analysis showed that the 56 core genes were significantly enriched in pathways such as "Bladder cancer," "Thyroid cancer," and "Melanoma"; For the Reactome pathway, the top three enriched were "AKT phosphorylates targets in the cytosol," "Apoptotic cleavage of cellular proteins," and "Apoptotic execution phase" (Supplementary Table 8). Next, we conducted PPI network analysis for the 56 genes. Results have revealed that the proteins encoded by these genes interact to a certain extent (142 edges/pairs in total), with the most robust interactions observed within a core cluster of 10 genes (40 edges/pairs): CDH1, MDM2, CCND1, AKT2, ZEB1, DNMT1, SP1, PGR, CDKN1A, and TP53 (Fig. 2C). Reactome pathway analysis showed the 10 genes were mainly enriched in 10 Reactome items, such as "AKT phosphorylates targets in the cytosol," "Transcriptional regulation by RUNX3," "Regulation of TP53 Expression and Degradation," and so on (Supplementary Table 8). Of the 13 identified common miRNAs, seven miRNAs seven miRNAs can target these 10 genes: hsa-miR-485-5p, hsa-miR-410-3p, hsa-miR-342-3p, hsa-let-7f-5p, hsa-miR-487a-3p, hsa-miR-194-5p, and hsa-miR-382-5p. Four of these seven miRNAs rank in the top five for the number of miRNA-target genes (hsa-miR-410-3p, hsa-miR-485-5p, hsa-miR-194-5p, hsa-let-7f-5p, and hsa-miR-342-3p).

GO and Pathway Enrichment Analysis of Common Genes

We conducted GO analysis and pathway enrichment analysis for the 56 common genes using the "clusterProfiler" package in R. The GO analysis encompassed three main domains: cellular component (CC), molecular function (MF), and biological process (BP); The pathway enrichment analysis used here incorporated enrichment results from both the KEGG and Reactome databases. The GO analysis results for these 56 genes revealed that the top five significantly enriched pathways at the BP level are "response to metal ion," "neuron death," "neuron apoptotic process," "regulation of neuron death," and "response to hypoxia"; At the CC level, the top five items are "membrane raft," "membrane microdomain," "platelet alpha granule lumen," "transcription

repressor complex," and "platelet alpha granule"; At the MF level, only three significantly enriched items were obtained, which are "histone deacetylase binding," "histone acetyltransferase binding," and "structural constituent of cytoskeleton" (Fig. 3A). The pathway enrichment analysis of the 56 genes yielded a total of 48 KEGG pathways and 43 Reactome pathways (Fig. 3B). The top five KEGG pathways are all associated with cancer: "Bladder cancer," "Thyroid cancer," "Melanoma," "p53 signaling pathway," and "Proteoglycans in cancer." The top five Reactome pathways are "AKT phosphorylates targets in the cytosol," "Apoptotic cleavage of cellular proteins," "Apoptotic execution phase," "Constitutive Signaling by AKT1 E17K in Cancer," and "Apoptosis." Detailed results for GO analysis and pathway enrichment analysis are shown in Supplementary Table 8.

Construction of the ERα-miRNA-mRNA Network

In the preceding analyses, a total of 13 target miRNAs and 56 target genes (target mRNAs) of ERα were identified using various bioinformatics approaches. Herein, we endeavored to construct FFL networks centered around ERα, leveraging the interrelationships among these elements (Fig. 4A). To enhance clarity in the whole FFL network's hierarchy, we omitted the interactions between target genes within the network. The 13 miRNAs were ordered according to the number of target mRNAs they possess, as follows: hsa-miR-410-3p (20 mRNAs), hsa-miR-485-5p (16 mRNAs), hsa-miR-194-5p (13 mRNAs), hsa-let-7f-5p (10 mRNAs), hsa-miR-342-3p (7 mRNAs), hsa-miR-25-3p (6 mRNAs), hsa-miR-425-5p (6 mRNAs),

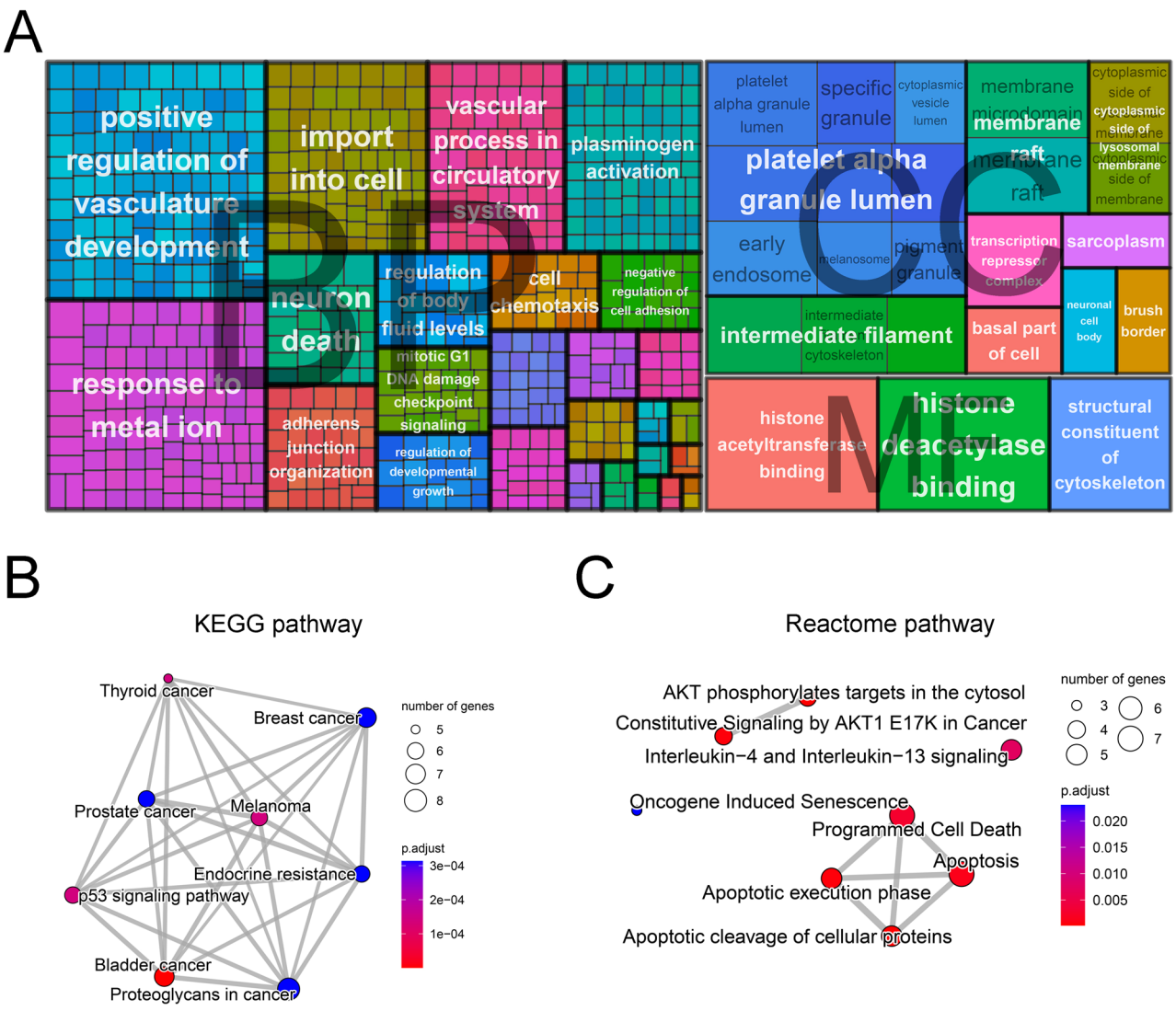

Fig. 3 Gene ontology and pathway enrichment analysis for the 56 common genes. **A** Gene ontology (GO) analysis results of the 56 common genes, categorized under cellular component (CC), molecular function (MF), and biological process (BP). **B–C** Pathway enrichment analysis showing the significant involvement of these genes in various KEGG or Reactome pathways

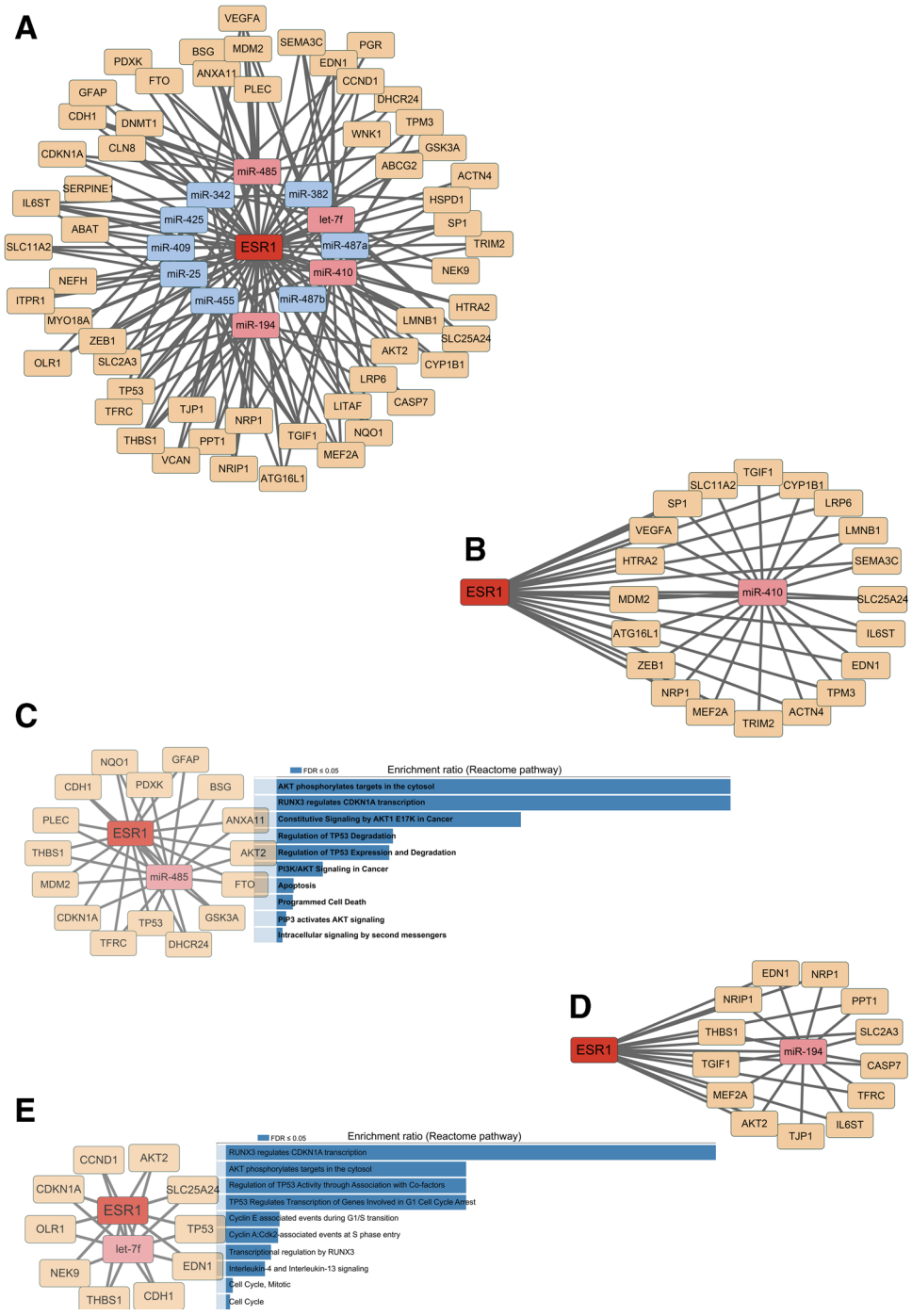

Fig. 4 ERα-miRNA-mRNA feed-forward loop (FFL) network construction. **A** Overview of the constructed ERα-miRNA-mRNA FFL network, highlighting the interplay among 13 miRNAs and 56 target genes. **B–D** Subnetworks for the top four miRNAs (hsa-miR-410-3p, hsa-miR-485-5p, hsa-miR-194-5p, hsa-let-7f-5p) based on the number of target mRNAs, with significant Reactome pathway enrichment observed for the subnetworks associated with miR-485-5p and let-7f-5p

hsa-miR-455-5p (6 mRNAs), hsa-miR-382-5p (5 mRNAs), hsa-miR-487a-3p (4 mRNAs), hsa-miR-409-5p (only 1 target mRNA), and hsa-miR-487b-3p (only 1 target mRNA). For visualization purposes, subnetworks of the first four miRNAs were extracted from the FFL network and displayed beneath the main network (Fig. 4B–D). Individual Reactome pathway enrichment analyses were conducted for each of the 13 subnetworks, revealing significant enrichment results for only two subnetworks: ERα/hsa-miR-485-5p and ERα/hsa-let-7f-5p. Interestingly, the genes within these two subnetworks were predominantly enriched in pathways related to AKT and RUNX3 (Fig. 4C, E and Supplementary Table 8). Upon further comparison, we found that these two subnetworks significantly overlapped with the PPI core cluster network, each containing five genes from the PPI core cluster, representing a 50% overlap of the genes within the PPI core cluster (Supplementary Table 8). This suggests that the

ERα/hsa-miR-485-5p and ERα/hsa-let-7f-5p subnetworks may play a crucial role in the overall regulatory network of ERα.

Discussion

This study focused on the aberrant regulation of ERα-miRNAs in the hippocampal region of AD and attempted to analyze the FFL networks of ERα. Firstly, we identified 70 abnormally expressed miRNAs and 1,617 important genes in the AD hippocampus through PubMed searching and the GeneCards database. Subsequently, we utilized multiple bioinformatics tools to predict target miRNAs and protein-coding genes downstream of ERα. Finally, we successfully constructed a whole ERα-miRNA-mRNA FFL network that includes 13 miRNAs and 56 genes.

The downstream regulatory network of ERα is highly complex, and its expression changes within the AD brain are also intricate, potentially exhibiting region- and cell-type-specificity [32]. Studies have found that compared to healthy brains matched for gender and age, ERα expression is increased in the hypothalamic infundibular nucleus (INF), medial mamillary nucleus (MMN), nucleus basalis of Meynert (NBM), and vertical limb of the diagonal band of Broca (VDB) of AD patients [33–36], while decreased in neurons of the hippocampus [37]. Another study found that the percentage of ERα-immunoreactive astrocytes in the hippocampus of AD patients is significantly higher than the control group [38], suggesting ERα regulation of astrocytes, which our results also corroborate to some extent. Our findings indicate an association between ERα and the astrocyte-specific marker GFAP in the final network (Fig. 4C).

There have been inconsistent reports regarding the impact of ERα on AD pathology, such as its effects on tau phosphorylation—some studies show that overexpression of ERα increases tau phosphorylation, while others report a decrease [5, 39, 40]. These inconsistencies further highlight the complexity of the ERα regulatory network. Moreover, at the transcription level, ERα can either enhance or inhibit the transcription of its target genes, influenced by various factors and involving numerous estrogen coregulators [41]. Considering these factors, the present study did not solely discard upregulated or downregulated miRNAs when searching for differentially expressed miRNAs in AD but included all of them in subsequent network construction. It has been shown that a large number of miRNAs are regulated by estrogen and its receptors in many tissues and cell types, such as uterine smooth muscle cells, human breast cancer cells, and mammary gland [42]. Our previous studies found that overexpression of ERα increases the expression of miR-218, thereby promoting AD pathology [5]. In SH-SY5Y cells, treatment with estradiol upregulates the expression of miR-106b-5p, which in turn protects these cells against $A\beta_{42}$-induced toxicity [43]. ERα is widely expressed in the hippocampus, which is one of the key regions affected by AD [44, 45]. The hippocampus region is also enriched with numerous miRNAs, some of which have been found to be dysregulated in AD [46]. Therefore, in the hippocampus, ERα may potentially regulate multiple miRNAs, thereby affecting downstream target genes and being involved in AD pathogenesis.

In the final network constructed, genes in the subnetwork of miR-485 and let-7f were both significantly enriched in pathways related to AKT, RUNX3, and TP53, as well as apoptosis-related signaling pathways. Actually, seven out of the 56 key genes are associated with the AKT pathway, and almost all of these seven genes were concentrated in the subnetwork of miR-485 and let-7f. The seven genes were AKT2, CCND1, CDKN1A, GSK3A, MDM2, THBS1, TP53, and VEGFA. AKT-associated pathways that the seven genes were enriched in were: KEGG item hsa04151 (PI3K-Akt signaling pathway); Reactome item R-HSA-198323 (AKT phosphorylates targets in the cytosol); Reactome item R-HSA-5674400 (Constitutive Signaling by AKT1 E17K in Cancer) and Reactome item R-HSA-2219528 (PI3K/AKT Signaling in Cancer) (Supplementary Table 8). Given that AKT signaling pathways are significantly dysregulated in AD [47], ERα may influence these molecules, thereby disrupting the AKT signaling pathway and participating in AD pathologies. This aligns with recent work by Chowdhury et al. [48], which underscores the role of estrogen dysregulation in exacerbating AD pathology through the modulation of shared metabolic pathways and key genes, such as PI3K, AKT, MAPK1, and KRAS.

The expression differences of ERα between males and females is also an important factor here [49, 50], which may also partially contribute to the morbidity of AD. Studies have shown that the expression and function of brain ERα can differ between males and females, with higher expression levels observed in females [49, 50]. Additionally, during menopause, there is a significant decline in estrogen levels, which may affect the expression of ERα [44, 51]. Consequently, the regulation of miRNAs and downstream target genes by ERα is not static; it can change at specific times, particularly during hormonal fluctuations associated with menopause, and these changes could potentially be involved in the pathogenesis of AD.

The present study has several limitations, the primary one being the lack of in vitro and in vivo validations. Our results and findings are based on computational methods and existing online databases. Although these methods and databases are robust, they do not provide the same level of empirical evidence as biological experiments. Additionally, there is the possibility of false positives and false negatives in bioinformatics predictions. Despite using multiple databases

and tools to predict target genes and miRNAs, the accuracy of these predictions may vary. Some predicted interactions may not be biologically relevant, and some true interactions may be missed. Furthermore, our study focuses solely on the hippocampus, which is a key area affected by AD. However, the brain is a complex organ, and the ERα-miRNA cross-talk may differ in other regions.

In conclusion, this study investigates the abnormal ERα-miRNA cross-talk in AD, revealing the complexity of the estrogen receptor regulatory network. More in vivo and in vitro experiments are needed to validate the findings, and a broader range of brain regions should be considered to gain a more comprehensive understanding of the abnormal ERα-miRNA cross-talk in AD.

Supplementary Information The online version contains supplementary material available at https://doi.org/10.1007/s12035-025-04771-2.

Author Contributions FFL: Conceptualization, Project administration, Funding acquisition, Writing – original draft, Writing – review & editing. KL: Conceptualization, Methodology, Funding acquisition, Supervision, Writing – review & editing.

Funding This study was partially supported by grants from the National Natural Science Foundation of China (Grant No. 81901103), and Wuhan Municipal Health Commission (Grant No. WX20Q14).

Data Availability No datasets were generated or analysed during the current study.

Code Availability Custom code used in the current study are available from the corresponding authors upon request.

Declarations

Competing Interests The authors declare no competing interests.

References

1. Scheltens P, De Strooper B, Kivipelto M, Holstege H, Chetelat G, Teunissen CE, Cummings J, van der Flier WM (2021) Alzheimer's disease. Lancet 397(10284):1577–1590. https://doi.org/10.1016/S0140-6736(20)32205-4
2. Mielke MM, Vemuri P, Rocca WA (2014) Clinical epidemiology of Alzheimer's disease: assessing sex and gender differences. Clin Epidemiol 6:37–48. https://doi.org/10.2147/CLEP.S37929
3. Toro CA, Zhang L, Cao J, Cai D (2019) Sex differences in Alzheimer's disease: understanding the molecular impact. Brain Res 1719:194–207. https://doi.org/10.1016/j.brainres.2019.05.031
4. Uddin MS, Rahman MM, Jakaria M, Rahman MS, Hossain MS, Islam A, Ahmed M, Mathew B, Omar UM et al (2020) Estrogen signaling in Alzheimer's disease: molecular insights and therapeutic targets for Alzheimer's dementia. Mol Neurobiol 57(6):2654–2670. https://doi.org/10.1007/s12035-020-01911-8
5. Xiong YS, Liu FF, Liu D, Huang HZ, Wei N, Tan L, Chen JG, Man HY, Gong CX, Lu Y, Wang JZ, Zhu LQ (2015) Opposite effects of two estrogen receptors on tau phosphorylation through disparate effects on the miR-218/PTPA pathway. Aging Cell 14(5):867–877. https://doi.org/10.1111/acel.12366
6. Jia M, Dahlman-Wright K, Gustafsson JA (2015) Estrogen receptor alpha and beta in health and disease. Best Pract Res Clin Endocrinol Metab 29(4):557–568. https://doi.org/10.1016/j.beem.2015.04.008
7. Tsang J, Zhu J, van Oudenaarden A (2007) MicroRNA-mediated feedback and feedforward loops are recurrent network motifs in mammals. Mol Cell 26(5):753–767. https://doi.org/10.1016/j.molcel.2007.05.018
8. Ivey KN, Srivastava D (2015) microRNAs as developmental regulators. Cold Spring Harb Perspect Biol 7(7):a008144. https://doi.org/10.1101/cshperspect.a008144
9. Shalgi R, Brosh R, Oren M, Pilpel Y, Rotter V (2009) Coupling transcriptional and post-transcriptional miRNA regulation in the control of cell fate. Aging (Albany NY) 1(9):762–770. https://doi.org/10.18632/aging.100085
10. Stelzer G, Rosen N, Plaschkes I, Zimmerman S, Twik M, Fishilevich S, Stein TI, Nudel R et al (2016) The GeneCards suite: from gene data mining to disease genome sequence analyses. Curr Protoc Bioinformatics 54(1):30. https://doi.org/10.1002/cpbi.5
11. Castro-Mondragon JA, Riudavets-Puig R, Rauluseviciute I, Lemma RB, Turchi L, Blanc-Mathieu R, Lucas J, Boddie P et al (2022) JASPAR 2022: the 9th release of the open-access database of transcription factor binding profiles. Nucleic Acids Res 50(D1):D165–D173. https://doi.org/10.1093/nar/gkab1113
12. Zhang Q, Liu W, Zhang HM, Xie GY, Miao YR, Xia M, Guo AY (2020) hTFtarget: a comprehensive database for regulations of human transcription factors and their targets. Genom Proteom Bioinform 18(2):120–128. https://doi.org/10.1016/j.gpb.2019.09.006
13. Consortium EP (2011) A user's guide to the encyclopedia of DNA elements (ENCODE). PLoS Biol 9(4):e1001046. https://doi.org/10.1371/journal.pbio.1001046
14. Han H, Shim H, Shin D, Shim JE, Ko Y, Shin J, Kim H, Cho A et al (2015) TRRUST: a reference database of human transcriptional regulatory interactions. Sci Rep 5:11432. https://doi.org/10.1038/srep11432
15. Tong Z, Cui Q, Wang J, Zhou Y (2019) TransmiR v2.0: an updated transcription factor-microRNA regulation database. Nucleic Acids Res 47(D1):D253–D258. https://doi.org/10.1093/nar/gky1023
16. Hua X, Tang R, Xu X, Wang Z, Xu Q, Chen L, Wingender E, Li J, Zhang C, Wang J (2018) mirTrans: a resource of transcriptional regulation on microRNAs for human cell lines. Nucleic Acids Res 46(D1):D168–D174. https://doi.org/10.1093/nar/gkx996
17. Miranda KC, Huynh T, Tay Y, Ang YS, Tam WL, Thomson AM, Lim B, Rigoutsos I (2006) A pattern-based method for the identification of MicroRNA binding sites and their corresponding heteroduplexes. Cell 126(6):1203–1217. https://doi.org/10.1016/j.cell.2006.07.031
18. Tastsoglou S, Alexiou A, Karagkouni D, Skoufos G, Zacharopoulou E, Hatzigeorgiou AG (2023) DIANA-microT 2023: including predicted targets of virally encoded miRNAs. Nucleic Acids Res 51(W1):W148–W153. https://doi.org/10.1093/nar/gkad283
19 Betel D, Wilson M, Gabow A, Marks DS, Sander C (2008) The microRNA.org resource: targets and expression. Nucleic Acids Res 36:D149-153. https://doi.org/10.1093/nar/gkm995

20 McGeary SE, Lin KS, Shi CY, Pham TM, Bisaria N, Kelley GM, Bartel DP (2019) The biochemical basis of microRNA targeting efficacy. Science 366:6472. https://doi.org/10.1126/science.aav1741

21. Vejnar CE, Blum M, Zdobnov EM (2013) miRmap web: comprehensive microRNA target prediction online. Nucleic Acids Res 41 (Web Server issue):W165–168. https://doi.org/10.1093/nar/gkt430

22. Kertesz M, Iovino N, Unnerstall U, Gaul U, Segal E (2007) The role of site accessibility in microRNA target recognition. Nat Genet 39(10):1278–1284. https://doi.org/10.1038/ng2135

23. Krek A, Grun D, Poy MN, Wolf R, Rosenberg L, Epstein EJ, MacMenamin P, da Piedade I et al (2005) Combinatorial microRNA target predictions. Nat Genet 37(5):495–500. https://doi.org/10.1038/ng1536

24. Szklarczyk D, Kirsch R, Koutrouli M, Nastou K, Mehryary F, Hachilif R, Gable AL, Fang T et al (2023) The STRING database in 2023: protein-protein association networks and functional enrichment analyses for any sequenced genome of interest. Nucleic Acids Res 51(D1):D638–D646. https://doi.org/10.1093/nar/gkac1000

25. Shannon P, Markiel A, Ozier O, Baliga NS, Wang JT, Ramage D, Amin N, Schwikowski B et al (2003) Cytoscape: a software environment for integrated models of biomolecular interaction networks. Genome Res 13(11):2498–2504. https://doi.org/10.1101/gr.1239303

26. Wu T, Hu E, Xu S, Chen M, Guo P, Dai Z, Feng T, Zhou L, Tang W et al (2021) clusterProfiler 4.0: a universal enrichment tool for interpreting omics data. Innovation (Camb) 2(3):100141. https://doi.org/10.1016/j.xinn.2021.100141

27. Ali A, Ajil A, MeenakshiSundaram A, Joseph N (2023) Detection of gene ontology clusters using biclustering algorithms. SN Computer Science 4(3):217. https://doi.org/10.1007/s42979-022-01624-w

28. Ali A, Hulipalled VR, Patil SS, Abdulkader R (2021) DPEBic: detecting essential proteins in gene expressions using encoding and biclustering algorithm. J Ambient Intell Humaniz Comput. https://doi.org/10.1007/s12652-021-03036-9

29. Yu G, He QY (2016) ReactomePA: an R/Bioconductor package for reactome pathway analysis and visualization. Mol Biosyst 12(2):477–479. https://doi.org/10.1039/c5mb00663e

30. Liao Y, Wang J, Jaehnig EJ, Shi Z, Zhang B (2019) WebGestalt 2019: gene set analysis toolkit with revamped UIs and APIs. Nucleic Acids Res 47(W1):W199–W205. https://doi.org/10.1093/nar/gkz401

31. Sayols S (2023) rrvgo: a bioconductor package for interpreting lists of Gene Ontology terms. MicroPubl Biol 2023. https://doi.org/10.17912/micropub.biology.000811

32 Hwang WJ, Lee TY, Kim NS, Kwon JS (2020) The role of estrogen receptors and their signaling across psychiatric disorders. Int J Mol Sci 22(1):373. https://doi.org/10.3390/ijms22010373

33. Hestiantoro A, Swaab DF (2004) Changes in estrogen receptor-alpha and -beta in the infundibular nucleus of the human hypothalamus are related to the occurrence of Alzheimer's disease neuropathology. J Clin Endocrinol Metab 89(4):1912–1925. https://doi.org/10.1210/jc.2003-030862

34. Ishunina TA, Kamphorst W, Swaab DF (2003) Changes in metabolic activity and estrogen receptors in the human medial mamillary nucleus: relation to sex, aging and Alzheimer's disease. Neurobiol Aging 24(6):817–828. https://doi.org/10.1016/s0197-4580(03)00009-5

35. Ishunina TA, Swaab DF (2001) Increased expression of estrogen receptor alpha and beta in the nucleus basalis of Meynert in Alzheimer's disease. Neurobiol Aging 22(3):417–426. https://doi.org/10.1016/s0197-4580(00)00255-4

36. Ishunina TA, Swaab DF (2003) Increased neuronal metabolic activity and estrogen receptors in the vertical limb of the diagonal band of Broca in Alzheimer's disease: relation to sex and aging. Exp Neurol 183(1):159–172. https://doi.org/10.1016/s0014-4886(03)00138-9

37. Hu XY, Qin S, Lu YP, Ravid R, Swaab DF, Zhou JN (2003) Decreased estrogen receptor-alpha expression in hippocampal neurons in relation to hyperphosphorylated tau in Alzheimer patients. Acta Neuropathol 106(3):213–220. https://doi.org/10.1007/s00401-003-0720-3

38. Lu YP, Zeng M, Hu XY, Xu H, Swaab DF, Ravid R, Zhou JN (2003) Estrogen receptor alpha-immunoreactive astrocytes are increased in the hippocampus in Alzheimer's disease. Exp Neurol 183(2):482–488. https://doi.org/10.1016/s0014-4886(03)00205-x

39. Bryant DN, Dorsa DM (2010) Roles of estrogen receptors alpha and beta in sexually dimorphic neuroprotection against glutamate toxicity. Neuroscience 170(4):1261–1269. https://doi.org/10.1016/j.neuroscience.2010.08.019

40. Wang C, Zhang F, Jiang S, Siedlak SL, Shen L, Perry G, Wang X, Tang B, Zhu X (2016) Estrogen receptor-alpha is localized to neurofibrillary tangles in Alzheimer's disease. Sci Rep 6:20352. https://doi.org/10.1038/srep20352

41. Fuentes N, Silveyra P (2019) Estrogen receptor signaling mechanisms. Adv Protein Chem Struct Biol 116:135–170. https://doi.org/10.1016/bs.apcsb.2019.01.001

42. Klinge CM (2009) Estrogen regulation of MicroRNA expression. Curr Genomics 10(3):169–183. https://doi.org/10.2174/1389202097881852 89

43. Pan Q, Guo K, Xue M, Tu Q (2021) Estradiol exerts a neuroprotective effect on SH-SY5Y cells through the miR-106b-5p/TXNIP axis. J Biochem Mol Toxicol 35(9):e22861. https://doi.org/10.1002/jbt.22861

44. Maioli S, Leander K, Nilsson P, Nalvarte I (2021) Estrogen receptors and the aging brain. Essays Biochem 65(6):913–925. https://doi.org/10.1042/EBC20200162

45. Schaub CE, Gersting JA, Keller-Wood M, Wood CE (2008) Development of ER-alpha and ER-beta expression in the developing ovine brain and pituitary. Gene Expr Patterns 8(6):457–463. https://doi.org/10.1016/j.gep.2008.03.001

46 Lukiw WJ (2023) MicroRNA (miRNA) complexity in Alzheimer's disease (AD). Biology (Basel) 12(6):788. https://doi.org/10.3390/biology12060788

47. Razani E, Pourbagheri-Sigaroodi A, Safaroghli-Azar A, Zoghi A, Shanaki-Bavarsad M, Bashash D (2021) The PI3K/Akt signaling axis in Alzheimer's disease: a valuable target to stimulate or suppress? Cell Stress Chaperones 26(6):871–887. https://doi.org/10.1007/s12192-021-01231-3

48. Chowdhury MR, Kumar V, Deepa VS (2024) Unraveling metabolic pathways and key genes in Alzheimer's, type 2 diabetes, and estrogen dysregulation among aging women: a systems biology approach. J Prot Proteom 15(3):347–360. https://doi.org/10.1007/s42485-024-00157-5

49. Lana LC, Hatsukano T, Sano K, Nakata M, Ogawa S (2023) Sex and age differences in the distribution of estrogen receptors in mice. Neurosci Lett 793:136973. https://doi.org/10.1016/j.neulet.2022.136973

50. Wilson ME, Westberry JM, Trout AL (2011) Estrogen receptor-alpha gene expression in the cortex: sex differences during development and in adulthood. Horm Behav 59(3):353–357. https://doi.org/10.1016/j.yhbeh.2010.08.004

51. Mosconi L, Nerattini M, Matthews DC, Jett S, Andy C, Williams S, Yepez CB, Zarate C et al (2024) In vivo brain estrogen receptor density by neuroendocrine aging and relationships with cognition and symptomatology. Sci Rep 14(1):12680. https://doi.org/10.1038/s41598-024-62820-7